

# Understanding the $2p$ core-level spectra of manganese: Photoelectron spectroscopy experiments and Anderson impurity model calculations

A. K. Shukla,<sup>1</sup> P. Krüger,<sup>2</sup> R. S. Dhaka,<sup>1</sup> D. I. Sayago,<sup>3</sup> K. Horn,<sup>3</sup> and S. R. Barman<sup>1</sup><sup>1</sup>UGC-DAE Consortium for Scientific Research, Khandwa Road, Indore, 452017 Madhya Pradesh, India<sup>2</sup>Institut Carnot de Bourgogne, UMR 5209 CNRS, Université de Bourgogne, 21078 Dijon, France<sup>3</sup>Fritz-Haber-Institut der Max-Planck-Gesellschaft, 14195 Berlin, Germany

(Received 25 January 2007; revised manuscript received 23 March 2007; published 14 June 2007)

Using high-resolution core-level photoelectron spectroscopy and modified Anderson impurity model calculations, we study the Mn  $2p$  spectrum of manganese metal and resolve the current debate about its spectral shape. An unusual satellite feature, 1 eV from the main peak, is observed in the Mn  $2p_{3/2}$  spectrum of a thick Mn layer grown on Al. It originates from intra-atomic multiplet effect related to Mn atoms with large local moment. The satellite decreases in intensity for thin Mn layers and for Al deposition on bulklike Mn because of enhanced Mn  $3d$  hybridization with Al  $s, p$  bandlike states. The reason for the absence of a charge-transfer satellite is discussed.

DOI: 10.1103/PhysRevB.75.235419

PACS number(s): 79.60.Dp, 73.61.At, 75.70.Ak

## I. INTRODUCTION

In the past two decades, extensive work has been performed to understand the electronic structure of different Mn-based compounds such as manganites, dilute magnetic semiconductors, quasicrystals, etc. It is very surprising that despite these efforts, the electronic structure of Mn metal is not fully understood to date.<sup>1-6</sup> Thus, a study of the Mn core levels and the  $2p$  spectrum, in particular, is of current interest, especially in view of the recent debate about its satellite structure.<sup>1-6</sup>

A correlation-induced charge-transfer satellite has been observed in Mn  $2p$  spectra of Mn layers deposited on different transition metals at 4–5 eV higher binding energy (BE).<sup>1-3</sup> Recently, Sandell and Jaworowski observed a satellite at 1 eV higher BE in the Mn  $2p$  spectra of Mn/Pd(100) that was ascribed to nonlocal core-hole screening.<sup>4</sup> On the other hand, a pronounced asymmetry but no satellite was observed for bulk Mn and thick Mn layer on Ag(001).<sup>2,6</sup> Schieffer *et al.* attributed this to correlation effects, but no reasons were provided.<sup>2</sup> The possibility of a hidden multiplet structure to explain the asymmetry was mentioned but discarded in Ref. 6. In Mn-based ferromagnetic Heusler alloys, a satellite at 1–1.5 eV was assigned to the  $2p$  exchange splitting.<sup>7</sup> In contrast, in Al-Mn alloys, such as Al<sub>6</sub>Mn or Al-Pd-Mn quasicrystal, no satellite or pronounced Mn  $2p$  asymmetry was observed.<sup>6,8</sup>

In this paper, we provide a comprehensive understanding of the Mn  $2p$  spectral shape and resolve the current disagreement in literature. This is of immense relevance to the electronic structure of Mn. An unusual satellite feature at 1 eV higher BE from the main peak is observed. Both multiplet effect and core-hole screening have been incorporated in the Anderson impurity model calculations, based on which we show that the satellite originates from intra-atomic multiplet effect. Although multiplet features have been reported earlier for MnO and MnF<sub>2</sub>,<sup>9</sup> a multiplet-induced satellite in the  $2p$  spectrum of a transition metal has not been observed earlier.

## II. EXPERIMENTAL METHOD

The experiments were performed at the UE56/2-PGM1 beamline at BESSY using EA125 analyzer from Omicron

GmbH with an instrumental resolution of 375 meV. The base pressure of the experimental chamber was  $5 \times 10^{-11}$  mbar. Electropolished Al(111) substrate was cleaned by standard method.<sup>10</sup> Mn and Al (99.999% purity) layers were deposited from two water-cooled Knudsen-type effusion cells with the substrate held at room temperature, and layer-by-layer growth was observed.<sup>11,12</sup>

To determine the relative intensities and the line shapes, the Mn  $2p_{3/2}$  spectra were fitted using two Doniach-Šunjić (DS) functions,<sup>13</sup> corresponding to the main peak and the 1 eV satellite.<sup>6,8</sup> The intrinsic lifetime broadening of the core level ( $2\gamma$ ), the DS asymmetry parameter ( $\alpha$ ), intensities, peak positions, and the iterative background parameter are varied independently during fitting. The residual in Fig. 1 shows the good quality of the fit. The satellite to main peak intensity ratio, calculated from the area under the fitted curves, is about 0.19. Although varied independently, our

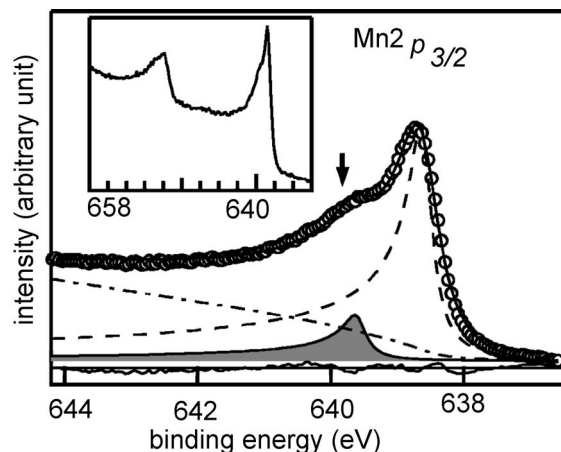


FIG. 1. Experimental (open circles) and fitted (solid line) Mn  $2p_{3/2}$  core-level spectra for a thick Mn layer on Al(111) recorded using 740 eV photon energy. The deconvoluted main peak (dashed line), the 1 eV satellite (shaded), the iterative background (dot-dashed), and the residual are shown. Inset shows both the Mn  $2p$  spin-orbit components.

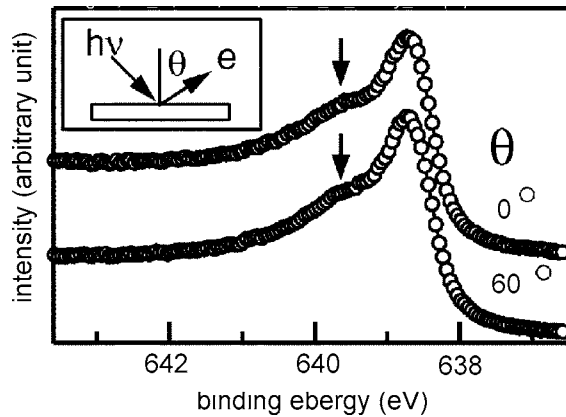


FIG. 2. Mn  $2p_{3/2}$  core-level spectra for a thick Mn layer grown on Al(111) as a function of emission angle ( $\theta$ ). The spectra have been shifted along the vertical axis for clarity of presentation. Inset shows the experimental geometry.

results yield a similar  $\alpha$  ( $=0.34 \pm 0.04$ ) for the main peak and the satellite, while  $\gamma$  turns out to be  $0.16 \pm 0.02$ .

### III. RESULTS AND DISCUSSION

#### A. Experiment: Core-level photoemission

The Mn  $2p$  core-level spectrum for a 44 monolayer (ML) thick bulklike Mn layer grown on Al(111) is shown in Fig. 1. Since the Mn layer is thick, no Al  $2p$  signal related to the substrate is observed. The Mn  $2p_{3/2}$  main peak appears at  $638.7 \pm 0.05$  eV (Fig. 1). A satellite feature (shown by arrow) is clearly observed at  $639.65$  eV, i.e.,  $\sim 1$  eV higher BE from the main peak. This feature is also observed for Mn thick layer on Al(100) (not shown). The inset in Fig. 1 shows the Mn  $2p$  spectrum with a spin-orbit splitting of  $11.2$  eV. This value is close to  $11.4$  eV spin-orbit splitting calculated for the Mn  $3d^6$  configuration.<sup>5</sup> Thus the main peak is dominated by the well-screened  $2p^5 3d^6$  final state.

In order to determine the origin of the 1 eV satellite, Mn  $2p_{3/2}$  spectra were recorded as a function of emission angle ( $\theta$ ) (Fig. 2). If the satellite is surface related, for example, a surface core-level shifted component or surface contamination, then it should be enhanced at grazing as compared to normal emission. However, the similarity of satellite (arrows in Fig. 2) for normal ( $\theta=0^\circ$ ) and nearly grazing emission ( $\theta=60^\circ$ ) rules out this possibility. Moreover, the surface core-level shift of Mn is expected to be less than  $0.3$  eV.<sup>14</sup>

The Mn adlayer on Al(111) with its several tens of monolayer thickness can be expected to take on the bulk structure of  $\alpha$ -Mn. Low-energy electron diffraction shows a uniform background with no spot from the thick layer, suggesting a polycrystalline growth.<sup>12</sup> Since the density of states (DOS) of the structurally inequivalent Mn atoms is similar in electron occupancy and hence effective valencies,<sup>15</sup> a chemical shift related to inequivalent Mn atoms cannot give rise to the 1 eV satellite. The satellite was not observed by Schieffer *et al.* for a thick (10 ML) Mn layer on Ag(001), possibly because of limited resolution ( $\approx 1$  eV for a Mg  $K\alpha$  source).<sup>2</sup> In

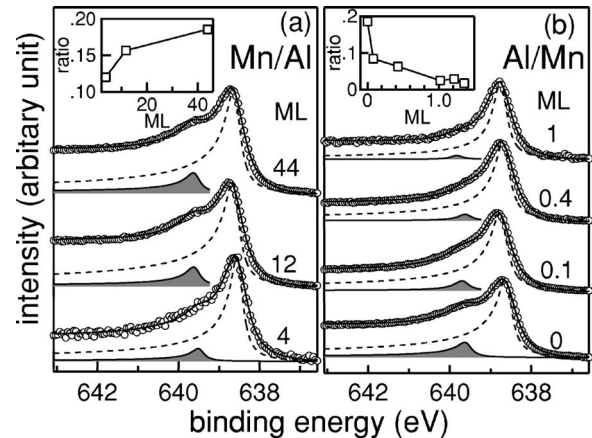


FIG. 3. Mn  $2p_{3/2}$  core-level spectra (open circles) for different coverages of (a) Mn on Al(111) and (b) Al on a bulklike Mn layer. The fitted spectra (thin solid line), the main peak (dashed line), and the satellite at 1 eV (shaded) obtained from least-squares fitting are shown. Insets show the satellite to main peak intensity ratio as a function of Mn coverage in (a) and Al coverage in (b).

order to confirm this, the Mn  $2p$  spectral shape, obtained by fitting the better resolution data (Fig. 1), was broadened by a fixed amount corresponding to our x-ray source and analyzer setting.<sup>10</sup> We obtain a highly asymmetric line shape that resembles the spectra in Refs. 2 and 6 and that recorded by us using Mg  $K\alpha$  for a thick Mn layer. If a single DS line shape is used to fit this asymmetric line shape, we obtain  $\alpha=0.49$ , which agrees with Ref. 6. The pronounced asymmetric line shape of Mn  $2p$  observed earlier<sup>2,6</sup> is thus related to the unresolved 1 eV satellite.

The above data suggest that the satellite at 1 eV is intrinsic to Mn electronic structure and hence, it is important to study its emergence as a function of film thickness [Fig. 3(a)]. For 4 ML Mn coverage, the satellite (shaded) is reduced in intensity compared to the thick layer (44 ML) (see inset). In a reverse experiment, Al was deposited on the bulklike Mn layer. Intriguingly, the satellite is strongly suppressed with increasing Al coverage and for about 1 ML coverage, it is almost nonexistent [Fig. 3(b), also see inset]. The position of the satellite, however, remains essentially unchanged. There is a gradual reduction in the asymmetry of the main line;  $\alpha$  decreases from 0.34 (0 ML) to 0.16 for 1.5 ML Al. Such small values of  $\alpha$  have been reported for  $\text{Al}_6\text{Mn}$  and  $\text{Al-Pd-Mn}$ .<sup>6,8</sup>

#### B. Theory: Model Hamiltonian calculations

We have performed impurity model calculations in order to ascertain the physical origin of the 1 eV satellite. Previously, we have calculated the Mn  $2p$  spectra for different Mn-Ag systems including bulk bct Mn.<sup>5</sup> The model used in Ref. 5 was tailored for ultrathin Mn films on Ag, where Mn has a high-spin, atomlike ground state. Here, we have used a somewhat different impurity model, which allows us to go continuously from an atomlike ground state to a bandlike ground state, where the spin is strongly reduced due to rapid charge fluctuations. The model describes one Mn atom

coupled to a metallic band. For simplicity, we take the limit of zero bandwidth, which means that the band is actually a reservoir of electrons and holes at the Fermi level ( $\epsilon_F$ ). The hybridization to the band is taken to be isotropic, and thus introduces a single parameter  $V$ . This way of treating charge fluctuations of the Mn 3d electrons is essentially the same as that used recently by Svane for Pu 5f electrons.<sup>16</sup>

The Hamiltonian is given by  $H = \epsilon_d n_d + \epsilon_F n_b + V \sum_{ms} (d_{ms}^\dagger b_{ms} + \text{H.c.}) + U_{dd} n_d (n_d - 1) / 2 - U_{dc} n_d \bar{n}_c + H_{\text{multiplet}}$ , where  $n_d$ ,  $n_b$ , and  $\bar{n}_c$  count the Mn d electrons, the band electrons, and the Mn 2p core hole, respectively. The operator  $d_{ms}^\dagger$  ( $b_{ms}^\dagger$ ) creates a d (band) electron of magnetic and spin quantum numbers  $m$  and  $s$ . The Hamiltonian above is exactly diagonalized in the subspace of  $d^4$ ,  $d^5$ ,  $d^6$ , and  $d^7$  configurations. The main differences to the model in Ref. 5 are (i) the band is taken to be non-spin-polarized, which is a good assumption for  $\alpha$ -Mn that is paramagnetic, and (ii) no restrictions on the number of holes and/or electrons in the band. By taking a total of ten valence electrons with as many up as down electrons in the ground state, all possible multiplet states of the configurations  $d^4$ ,  $d^5$ ,  $d^6$ , and  $d^7$  can mix through hopping in and out of the band. This is crucial for studying the crossover from an atomlike, high-spin ground state to a bandlike, low-spin one.

The parameters entering the multiplet part of the Hamiltonian were computed from single-ion Hartree-Fock calculations<sup>17</sup> in the  $(2p^5 3d^6)$  configuration, which is the dominant one in the final state. As usual, the values of the Slater integrals  $F^k$ ,  $G^k$  are reduced by 20%, while the bare value is taken for the 2p spin-orbit parameter  $\zeta_p$ . The 3d spin-orbit interaction has been neglected. This gives the following values:  $F_{dd}^2 = 8.92$ ,  $F_{dd}^4 = 5.55$ ,  $F_{pd}^2 = 5.06$ ,  $G_{pd}^1 = 3.69$ ,  $G_{pd}^3 = 2.09$ , and  $\zeta_p = 6.85$  (in eV).

For the monopole Coulomb integrals, we have taken the values  $U_{dd} = 3.0$  eV and  $U_{dc} = 4.12$  eV, as determined in Ref. 18. Putting  $\epsilon_F = 0$ , the d level  $\epsilon_d$  controls the ground-state d-electron number  $n_d$ . Equivalently, we can fix the charge-transfer energy  $\Delta$ , which we define as  $\Delta = E(d^6) - E(d^5)$ , where  $E(d^n)$  are configuration averaged energies. [Note that a  $(d^n)$  configuration should more precisely be denoted as  $(d^n b^{10-n})$ , but we have  $E(d^n b^{10-n}) = E(d^n)$ , since  $\epsilon_F = 0$ .] We have chosen  $\Delta = -2$  eV, which leads to  $n_d = 5.7 \pm 0.1$  for all  $V \geq 0.5$  eV. This  $n_d$  value agrees with first-principles calculations on bulk bct Mn.<sup>5</sup> All the theoretical spectra have been broadened with Gaussians and Lorentzians using the experimental full width at half maximum values.

Figure 4 shows the calculated Mn 2p spectra as a function of  $V$ . The spectra in solid lines were calculated with the parameter values as stated above, in particular,  $U_{dc} = 4.12$  eV. The spectra in broken lines were obtained with  $U_{dc} = 0$ . The spectrum labeled “0.0” is the atomic spectrum for  $n_d = 5$ .

We shall first discuss the results for  $U_{dc} = 4.12$  eV (solid lines). We concentrate on the  $2p_{3/2}$  part of the spectrum, which is found at the negative relative BE side in Fig. 4. One can roughly divide the  $2p_{3/2}$  spectrum into three groups of peaks, which we indicated by broken lines, labeled a, b, and c. Group a, which evolves continuously from the atomic spectrum, can be assigned to the  $(2p^5 3d^5)$  atomic configura-

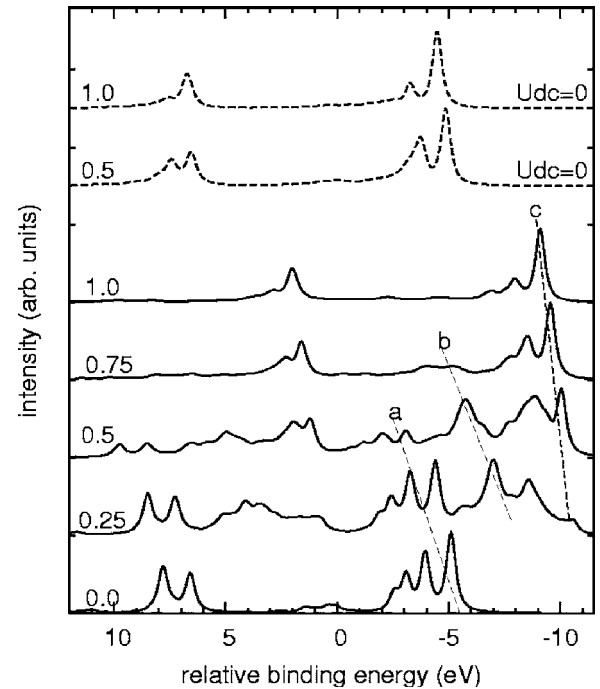


FIG. 4. Calculated Mn 2p photoemission spectra as a function of  $V$  (in eV) as indicated by the number on the left. The two uppermost spectra (broken lines), labeled  $U_{dc} = 0$ , were calculated with  $U_{dc} = 0$ . All other spectra (solid lines) were obtained with  $U_{dc} = 4.12$  eV. The spectra have been normalized to equal main peak intensity. The thin broken lines labeled a, b, and c are guides for the eyes.

tion. From energy considerations for  $V = 0$ , we may infer that groups b and c are dominantly due to  $(2p^5 3d^6)$  and  $(2p^5 3d^7)$  configurations, respectively. It is to be noted, however, that these assignments are very approximate and can only be valid for small values of  $V$ . With increasing  $V$ , configuration mixing becomes large, and no more simple assignments to atomic configurations can be made. Despite this, it is clear that the presence of more than one of the groups a, b, or c is due to the fact that final states with different d-electron counts can be reached. This means that the satellite structures a and b that are seen in the spectra for  $0 < V \leq 0.5$  eV are of charge-transfer type. Such strong charge-transfer satellites at 4–5 eV higher BE from the main line have been observed for ultrathin Mn layers on various transition or noble metal substrates.<sup>1–4</sup> The results in Fig. 4 show that charge-transfer satellites are only appreciable for small hybridization strengths,  $V < 0.75$ . In bulk Mn, as well as in Al/Mn and Al-Mn alloys,  $V$  can be estimated to be at least 1 eV (see below), which explains why the 4–5 eV charge-transfer satellite is not observed in these systems.

The spectra for  $V \geq 0.75$  eV, moreover, show a satellite at 1–1.5 eV higher BE from the main line, in agreement with the experimental spectra in Figs. 1–3. For easier comparison with experiment, we show the  $2p_{3/2}$  part of the calculated spectra in more detail in Fig. 5. Here, the spectra have been energy shifted such that the main peaks are aligned. The position of the satellite with respect to the main line is roughly constant. The inset in Fig. 5 shows the peak intensity ratio  $I_S$  between the 1 eV satellite and the main line, as a

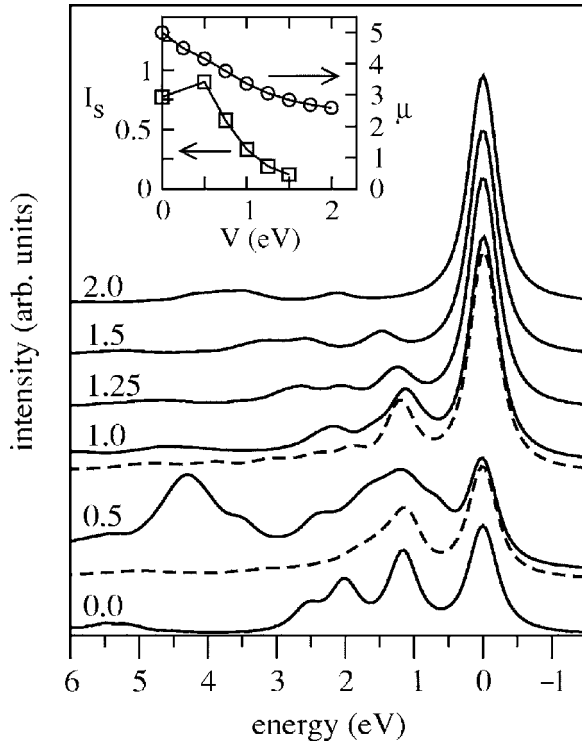


FIG. 5. Calculated Mn  $2p_{3/2}$  photoemission spectra as a function of  $V$  as indicated on the left (in eV). Solid lines correspond to the parameter values as given in the text, in particular,  $U_{dc}=4.12$  eV. The dashed lines correspond to  $U_{dc}=0$  and the same  $V$  as the solid lines just above. The maxima of the main peaks are aligned at zero energy. They are normalized such that the main peak has equal intensity for spectra with  $V \geq 1$  and half of that for  $V < 1$ . Inset shows the peak intensity ratio between the main line and the 1 eV satellite for the spectra with  $U_{dc}=4.12$  eV (squares, left y axis) as well as the ground-state isotropic spin moment  $\mu$  (circles, right y axis) as a function of  $V$ .

function of  $V$ . It can be seen that the satellite intensity decreases quickly in the range of  $0.5 < V < 1.5$  eV.

The value of  $V$  can be estimated to be about a quarter of the Mn  $d$  bandwidth  $W$ . This can be seen as follows: Since we have taken the limit of zero bandwidth for the *electron* and/or *hole reservoir*, the total system (impurity plus reservoir) has a simple two-level electronic structure with one bonding and one antibonding level separated by  $2V$ , assuming  $\epsilon_d = \epsilon_f$ . In order to relate  $V$  to  $W$ , we note that the second moment of the two-level system, which is  $V^2$ , should be equal to the second moment of the Mn  $d$  band. Assuming a semielliptic density of states for the band, its second moment is  $W^2/16$ . So  $V^2 = W^2/16$  or  $V = W/4$ .

In bulk  $\alpha$ -Mn,  $W$  is about 5–6 eV according to Ref. 15, which gives  $V \sim 1.2$ –1.5 eV. The spectrum for these  $V$  values agrees well with the experimental one for the bulklike Mn films (Fig. 1). The main difference is the lack of asymmetry in the calculated spectra. The observed asymmetry is due to core-hole screening by low-lying particle-hole excitations across  $\epsilon_f$ .<sup>13</sup> This effect is not correctly described in the present model, because of the limit of zero bandwidth.

The atomic Mn spectrum (curve 0.0 in Figs. 4 and 5) features a strong satellite at about 1.2 eV from the  $2p_{3/2}$  main

line. This suggests that the observed 1 eV satellite has an intra-atomic origin, i.e., it is a residual multiplet structure. The rich multiplet structure in the atomic spectrum is mainly due to the strong  $2p$ - $3d$  exchange interaction and to the high-spin ground state of atomic Mn. Band-structure calculations show that 17% of the Mn atoms in the  $\alpha$ -Mn unit cell have large moment ( $2.8$ – $3.2\mu_B$ ).<sup>15</sup> The good agreement between the fraction of Mn atoms with large moment (0.17) and the satellite to main peak intensity ratio (0.19) associates the 1 eV satellite with Mn atoms with large local moment.

In order to clarify this issue further, we now show that the 1 eV satellite intensity is strongly correlated with the local magnetic moment on the Mn atom. In the present impurity model, the ground state is a total spin singlet, for all  $V > 0$ . Therefore, the spin projection on the impurity atom  $\langle g|S_z|g \rangle$  is exactly zero along any quantization axis  $z$ . Here,  $S_z$  is the  $z$  component of the spin operator of the impurity  $d$  shell and  $|g \rangle$  is the ground state. The usual definition of the local (spin) magnetic moment,  $\mu_z = 2\langle g|S_z|g \rangle$ , is inappropriate for the present model, since it always yields zero. To monitor the local spin moment on the impurity, we need an isotropic quantity instead of  $\mu_z$ . Consider  $\langle g|S^2|g \rangle$  with  $\mathbf{S} = (S_x, S_y, S_z)$ . In the atomic limit,  $S^2 = S(S+1)$  is a good quantum number and the spin moment is given by  $\mu = 2S$ . Following these atomic relations, we define an isotropic spin moment  $\mu$  of the impurity through  $\mu(\mu+2)/4 = \langle g|S^2|g \rangle$ . Note that while this definition is exact for atomic systems, the values obtained for  $V \neq 0$  can be much bigger than the real magnetic moments. In the present case, we get  $\mu \approx 2$  in the limit  $V \rightarrow \infty$ , where the Mn atom is definitely nonmagnetic. Thus,  $\mu$  is only a semiquantitative measure of the magnetic moment on the Mn atom. The inset of Fig. 5 shows  $\mu$  as a function of  $V$ . The spin moment  $\mu$  decreases with  $V$ , because charge fluctuation reduces Hund's rule correlations, that is, the tendency for  $d$ -electron spins to align. In the range  $0.5 < V < 1.5$  eV, a clear positive correlation between the isotropic spin moment  $\mu$  and the satellite intensity  $I_s$  can be observed.

In order to definitively prove that the 1 eV satellite is a multiplet effect and not due to charge screening of the core hole, we have carried out a few calculations with  $U_{dc}=0$ . These are shown in Figs. 4 and 5 as dashed lines. When  $U_{dc}=0$ , the  $d$  level is not pulled down in the final state and so the core-hole screening effect is absent. Consequently, charge-transfer satellites cannot appear. This is nicely confirmed by the fact that the 4–5 eV charge-transfer satellite, which has large intensity in the spectrum for  $V=0.5$  and  $U_{dc}=4.12$ , is completely absent in the spectrum for  $V=0.5$  and  $U_{dc}=0$ . The 1 eV satellite, on the other hand, is present in both spectra. Also for  $V=1$  eV, the 1 eV satellite is hardly affected when going from  $U_{dc}=4.12$  to  $U_{dc}=0$ , but the small features at higher BE are suppressed. The comparison with the case  $U_{dc}=0$  thus clearly shows that the 1 eV satellite is not related to charge screening of the core hole and must therefore be due to an intra-atomic, that is, multiplet effect.

The present model contains four adjustable parameters,  $\Delta$ ,  $U_{dd}$ ,  $U_{dc}$ , and  $V$ . We have estimated them as well as possible by comparison either with other experimental data ( $U_{dd}$ ,  $U_{dc}$  see Ref. 18) or with *ab initio* electronic structure data ( $\Delta$ ,  $V$ ). Nonetheless, some uncertainty remains about the best choice

of the parameter values and, consequently, about the calculated line shape. While the charge-transfer satellite structures depend quite strongly on all four parameters, the 1 eV satellite is essentially independent of  $\Delta$ ,  $U_{dc}$ , and  $U_{dd}$ . For  $U_{dc}$ , this fact can directly be checked from Figs. 4 and 5. Therefore, the main conclusions of this work, which deal with the 1 eV satellite, are insensitive to the adjustable parameters except  $V$ . The dependence of the 1 eV satellite on  $V$  has been discussed in detail and provides a major result of the analysis.

Let us note that the  $2p$ - $3d$  exchange interaction has already been put forward by Plogmann *et al.* to explain 1–1.5 eV satellites observed in Mn  $2p_{3/2}$  x-ray photoemission spectroscopy of Heusler alloys.<sup>7</sup> Their theoretical analysis was based on the independent particle approximation (IPA). Here, we have reached a qualitatively similar explanation for the 1 eV satellite as in Ref. 7, namely, that it is due to  $2p$ - $3d$  exchange and thus a measure of the local magnetic moment on the Mn atoms. The line shapes obtained from our many-body calculations are, however, very different from those obtained in the IPA. In the IPA, the  $2p$ - $3d$  multiplet interaction is replaced by an effective magnetic field acting on the  $2p$  electrons, which results in an effective Zeeman effect. The  $2p_{3/2}$  level is then split into four equidistant lines, which have equal intensity in the isotropic photoemission spectrum. In that picture, the line *splitting* scales with the magnetic moment of the atom. Here, we come to a very different conclusion, namely, that it is the satellite *intensity* that scales roughly with the magnetic moment, while the main line to satellite splitting is fairly independent of it.

While the satellite has thus been identified as having an intra-atomic origin, its intensity strongly depends on the extra-atomic hybridization strength  $V$ . Our rough estimation of  $V \sim 1.2$ – $1.5$  eV, together with the spectra in Fig. 5, suggest that the  $V$  value appropriate for bulk Mn is rather close to the borderline at which the satellite vanishes. Our surprising experimental finding that the intensity of the 1 eV satellite decreases for Al deposition on Mn and for thin Mn adlayers may be understood as follows: For Al/Mn, the  $s$ - $d$  hybridization is enhanced because Al  $s$ ,  $p$  free-electron-like bands hybridize with the Mn  $3d$ ,  $4s$  bands through the over-

lap of the 11 eV wide parabolic DOS of Al with the Mn  $3d$  dominated DOS centered around 2.5 eV BE.<sup>15,19</sup> Thus, Al deposition definitely enhances  $V$ , and this diminishes the satellite intensity, as shown in Fig. 5. This also explains why Al-Mn alloys with substantial  $s$ - $d$  hybridization do not exhibit this satellite.<sup>6,8</sup>

#### IV. CONCLUSIONS

In conclusion, we provide a comprehensive understanding and resolve the existing incongruity in literature about the Mn  $2p$  spectral shape of manganese that is fundamental to its electronic structure. An unexpected satellite in the Mn  $2p_{3/2}$  spectrum of bulklike manganese layers at 1 eV higher BE is observed. The satellite is not related to surface effects or charge screening of the core hole. We show that it originates from intra-atomic multiplet effect associated with Mn atoms with large local moment. Its intensity is correlated with the local magnetic moment of Mn. Al deposition on Mn strongly suppresses the 1 eV satellite due to enhanced  $s$ - $d$  hybridization. The charge-transfer satellite at 4–5 eV can only exist for weak hybridization strengths, and so it is absent for bulk Mn. Hence, Al-Mn alloys including quasicrystals that have substantial  $s$ - $d$  hybridization do not exhibit any satellite in their Mn  $2p$  spectra. The present findings demonstrate the importance of multiplet interactions, which are generally considered to be insignificant.<sup>3</sup> Consequently, far reaching implications for the electronic structure of Mn-based compounds and correlated systems, in particular, might be expected, necessitating reinvestigation using high-resolution core-level photoelectron spectroscopy.

#### ACKNOWLEDGMENTS

We thank P. Chaddah, A. Gupta, and D. P. Woodruff for constant encouragement. W. Mahler and B. Zada are thanked for technical help. Funding from Max Planck Gesellschaft, Germany and Department of Science and Technology, India is gratefully acknowledged. AKS is thankful to Council for Scientific and Industrial Research, India for financial support.

<sup>1</sup>M. Wuttig, Y. Gauthier, and S. Blügel, Phys. Rev. Lett. **70**, 3619 (1993).

<sup>2</sup>P. Schieffer, C. Krembel, M. C. Hanf, and G. Gewinner, J. Electron Spectrosc. Relat. Phenom. **104**, 127 (1999); Phys. Rev. B **57**, 1141 (1998).

<sup>3</sup>O. Rader, W. Gudat, C. Carbone, E. Vescovo, S. Blügel, R. Kläsches, W. Eberhardt, M. Wuttig, J. Redinger, and F. J. Himpsel, Phys. Rev. B **55**, 5404 (1997); O. Rader, T. Mizokawa, A. Fujimori, and A. Kimura, *ibid.* **64**, 165414 (2001).

<sup>4</sup>A. Sandell and A. J. Jaworowski, J. Electron Spectrosc. Relat. Phenom. **135**, 7 (2004).

<sup>5</sup>P. Krüger and A. Kotani, Phys. Rev. B **68**, 035407 (2003).

<sup>6</sup>V. Fournée, J. W. Andereg, A. R. Ross, T. A. Lograsso, and P. A. Thiel, J. Phys.: Condens. Matter **14**, 2691 (2002).

<sup>7</sup>S. Plogmann, T. Schlathölder, J. Braun, M. Newmann, Y. M.

Yarmoshenko, M. Yablonskikh, E. I. Shreder, E. Z. Kurmaev, A. Wrona, and A. Ślebarski, Phys. Rev. B **60**, 6428 (1999).

<sup>8</sup>K. Horn, W. Theis, J. J. Paggel, S. R. Barman, E. Rotenberg, Ph. Ebert, and K. Urban, J. Phys.: Condens. Matter **18**, 435 (2006).

<sup>9</sup>B. Hermsmeier, C. S. Fadley, M. O. Krause, J. Jimenez-Mier, P. Gerard, and S. T. Manson, Phys. Rev. Lett. **61**, 2592 (1988).

<sup>10</sup>C. Biswas, A. K. Shukla, S. Banik, V. K. Ahire, and S. R. Barman, Phys. Rev. B **67**, 165416 (2003); C. Biswas, A. K. Shukla, S. Banik, S. R. Barman, and A. Chakrabarti, Phys. Rev. Lett. **92**, 115506 (2004).

<sup>11</sup>A. K. Shukla, S. Banik, R. S. Dhaka, C. Biswas, S. R. Barman, and H. Haak, Rev. Sci. Instrum. **75**, 4467 (2004).

<sup>12</sup>C. Biswas, R. S. Dhaka, A. K. Shukla, and S. R. Barman, Surf. Sci. **601**, 609 (2007).

<sup>13</sup>S. Doniach and M. Šunjić, J. Phys. C **3**, 287 (1970).

- <sup>14</sup>B. Johansson and N. Mårtensson, Phys. Rev. B **21**, 4427 (1980).
- <sup>15</sup>D. Hobbs, J. Hafner, and D. Spišák, Phys. Rev. B **68**, 014407 (2003).
- <sup>16</sup>A. Svane, Solid State Commun. **140**, 364 (2006). See  $\hat{H}_{\text{imp}}$ , Eqs. (3)–(5).
- <sup>17</sup>R. D. Cowan, *The Theory of Atomic Structure and Spectra* (University of California Press, Berkeley, 1981).
- <sup>18</sup>M. Taguchi, P. Krüger, J.-C. Parlebas, and A. Kotani, J. Phys. Soc. Jpn. **73**, 1347 (2004); Phys. Rev. B **73**, 125404 (2006).
- <sup>19</sup>Y. Baer and G. Busch, Phys. Rev. Lett. **30**, 280 (1973).